JACS Au
AN OPEN ACCESS JOURNAL OF THE AMERICAN CHEMICAL SOCIETY

pubs.acs.org/jacsau
Article

An Aptamer Glue Enables Hyperefficient Targeted Membrane Protein Degradation

Guo-Rong Zhang, Chi Zhang, Ting Fu, Weihong Tan, and Xue-Qiang Wang*

Cite This: *JACS Au* 2024, 4, 2907−2914
Read Online

ACCESS | Metrics & More | Article Recommendations | Supporting Information

ABSTRACT: Targeted membrane protein degradation (TMPD) offers significant therapeutic potential by enabling the removal of harmful membrane-anchored proteins and facilitating detailed studies of complex biological pathways. However, existing TMPD methodologies face challenges such as complex molecular architectures, scarce availability, and cumbersome construction requirements. To address these issues, this study presents a highly efficient TMPD system (TMPDS) that integrates an optimized bivalent aptamer glue with a potent protein transport shuttle. Utilizing this approach, we successfully degraded both the highly expressed protein tyrosine kinase 7 in CCRF-CEM cells and the poorly expressed PTK7 in MV-411 cells. This system represents significant advancement in the field of molecular medicine, offering a new avenue for targeted therapeutic interventions and the exploration of cellular mechanisms.

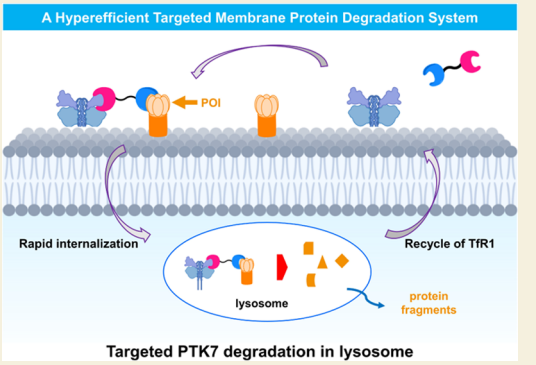

KEYWORDS: *aptamer, bispecific, aptamer glue, membrane protein, hyperefficient, targeted degradation*

Targeted membrane protein degradation (TMPD), as an innovative strategy in the protein manipulation area, offers the dual benefit of expanding the scope of pharmacological intervention and enabling comprehensive investigations of complex biological pathways. This approach employs a targeting-transport-degradation strategy to selectively deplete the membrane-anchored proteins of interest (MAPOI), thereby facilitating a comprehensive exploration of their roles and functions. Currently, only very few works, including lysosome-targeting chimeras (LYTACs),[1] covalent nanobody-based proteolysis targeting chimeras strategy (GlueTAC),[2] antibody-based PROTACs (AbTACs),[3] bispecific aptamer chimeras,[4] and aptamer-based LYTAC (Apt-LYTAC),[5] were designed. Nevertheless, it is particularly worth noting that it is necessary to incubate cells with high-concentration probes for 24−48 h to achieve significant degradation, implying their low degradation rate. To overcome this drawback, we herein report the design of a hyperefficient targeted membrane protein degradation system (TMPDS) that incorporates an optimized bivalent aptamer glue and a highly efficient protein transporting shuttle.

The transferrin receptor protein 1 (TfR1), also known as cluster of differentiation 71 (CD71), plays a vital role in the efficient uptake of iron from transferrin into lysosomes of cells through endocytosis.[6] Notably, TfR1 is frequently overex-

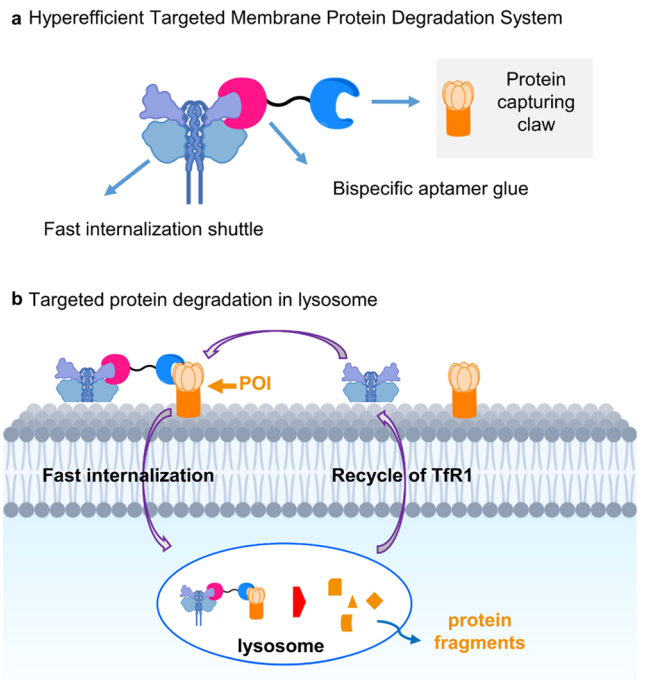

Figure 1. Designing a hyperefficient TMPDS. (a) Components of TMPDS. (b) Proposed catalytic cycle.

Received: March 21, 2024
Revised: May 17, 2024
Accepted: May 17, 2024
Published: August 8, 2024

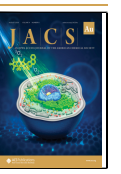

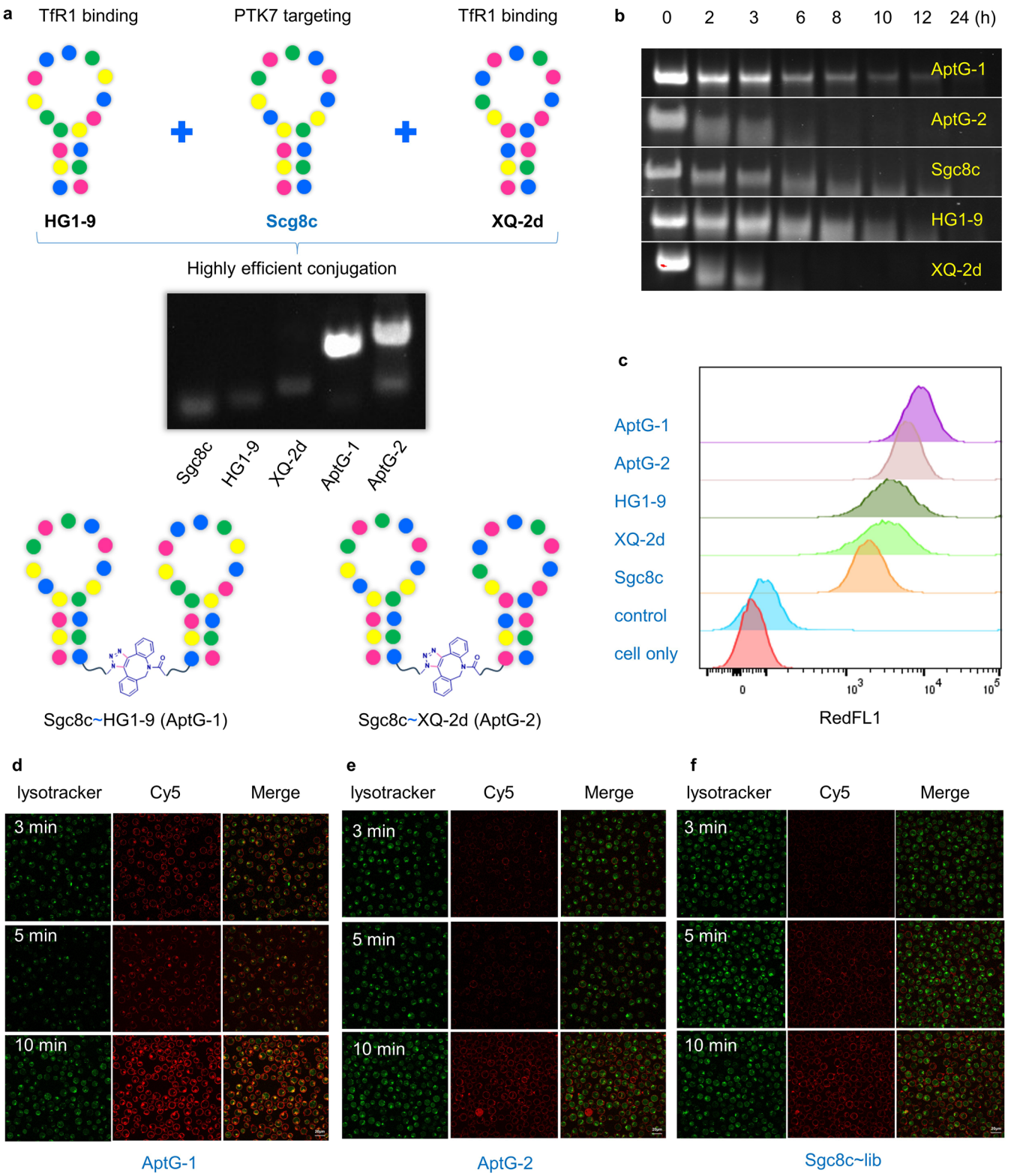

Figure 2. (a) Designing and highly efficient construction of AptG-1 and AptG-2. (b) Comparing the stability of the probes in 20% FBS for different times. (c) Binding ability analysis of the probes for CCRF-CEM at 4 °C. (d) Comparing the fluorescence intensity of CCRF-CEM treated with different concentrations of AptG-1, AptG-2, and Sgc8c~lib for 30 min at 4 °C. (d–f) Comparison of the internalization rate of AptG-1, AptG-2 and Sgc8c~lib at different time points, CCRF-CEM cells were incubated with 500 nM AptG-1, AptG-2, and Sgc8c~lib for 3, 5, or 10 min in cell culture medium at 37 °C.

pressed on the membrane of numerous cancer cell lines due to their elevated iron requirements.[6,7] These characteristics render TfR1 an ideal component for constructing highly efficient TMPDS (Figure 1a,b). On the other hand, the unique structure of the ligand binding to TfR1 is of utmost importance in the TMPDS as it governs the formation tendency of Aptamer Glue-

https://doi.org/10.1021/jacsau.4c00260
JACS Au 2024, 4, 2907−2914

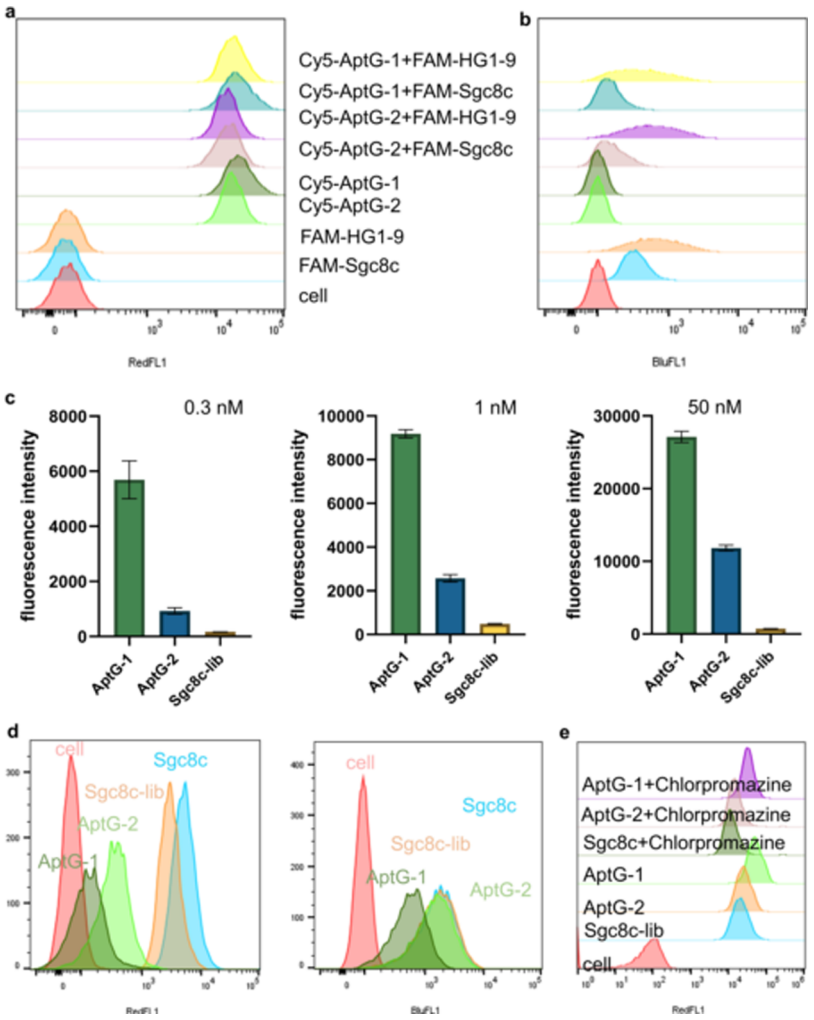

Figure 3. Mechanistic studies for a faster internalization rate of AptG-1. (a, b) Comparison of the binding ability rates of AptG-1, AptG-2, and Sgc8c∼lib, and monovalent aptamers. CCRF-CEM cells were incubated with 200 nM Cy5-AptG-1 and FAM-Sgc8c, 200 nM Cy5-AptG-1 and FAM-HG1−9, 200 nM Cy5-AptG-2 and FAM-Sgc8c, 200 nM Cy5-AptG-2 and FAM-HG1−9, 200 nM FAM-Sgc8c, 200 nM FAM-HG1−9, 200 nM Cy5-AptG-1, and 200 nM Cy5-AptG-2 for 30 min in binding buffer at 4 °C. (a) Cy5 fluorescent channel. (b) FAM fluorescent channel. (c) Comparison of the binding ability of AptG-1, AptG-2, and Sgc8c∼lib at extremely low concentrations. CCRF-CEM cells were incubated with 0.3, 1, and 50 nM AptG-1, AptG-2, and Sgc8c∼lib for 30 min in binding buffer at 4 °C. (d) Substitution experiments were conducted by co-incubating AptGs with CCRF-CEM at 4 °C for 30 min. CCRF-CEM cells were incubated with 200 nM AptG-1, AptG-2, and Sgc8c∼lib for 30 min in binding buffer at 4 °C, followed by labeling PTK7 receptor with Cy5-Sgc8c aptamer and labeling CD71 receptor with FAM-HG1−9 aptamer at 4 °C for 30 min. The treated cells were then subjected to binding with Cy5-labeled Sgc8c (right) and FAM-labeled HG1−9 (left). (e) Exploring the influence of the endocytosis pathways on the TMPDS. 50 μM chlorpromazine was incubated with Cy5-AptG-1, Cy5-AptG-2, and Cy5-Sgc8c at the concentration of 500 nM for 2 h.

TfR1 complexes, the subsequent internalization process, and the rate of transporting. In addition, the recognition ability and binding affinity of the protein of interesting (POI) capturing ligand, which serves as the final part of the TMPDS, are crucial factors that influence the degradation efficiency by dictating the capture of the MAPOI.

With these considerations in mind, our investigation commenced with the design of aptamer glues (AptGs) that comprise a TfR1 binding aptamer and a MAPOI apprehending aptamer. Recognizing the crucial role of the TfR1 binding aptamer in determining the transport rate, we utilized either XQ-2d[8] or HG1−9[9] as an additional critical component to construct AptGs for further optimization investigations (Figure 2a). An array of studies have demonstrated that PTK7 (Tyrosine-protein kinase-like 7) plays important roles as a context-dependent signaling switch for the Wnt pathways,[10] Sgc8c was thus selected as the MAPOI targeting aptamer.[11] High conjugation efficiency was achieved for both AptG-1 (Sgc8c ∼ HG1−9) and AptG-2 (Sgc8c ∼ XQ-2d), as shown in Figure 2a, and almost quantitative yield was observed for AptG-1.[12] Next, the enzyme degradation resistance ability of these probes was investigated. Incubation of AptG-1, AptG-2, Sgc8c, HG1−9, and XQ-2d for the appointed time at 37 °C allowed us to observe the superior stability of AptG-1 in 1640 culture media over the other probes, which is a crucial parameter for TMPD application (Figure 2b).

To evaluate the recognition ability of these probes against targeted cell lines, we selected the CCRF-CEM cell line to perform flow cytometry assays (Figure 2c) and found that AptG-1 exhibited significantly better recognition ability compared to AptG-2. These results prompted us to further compare the endocytosis ability of AptG-1 with AptG-2 using Sgc8c ∼ lib as a control sample (Figure 2d versus e and 2f). Remarkably, AptG-1 demonstrated a much faster internalization rate. Cy5-labeled

https://doi.org/10.1021/jacsau.4c00260
JACS Au 2024, 4, 2907−2914

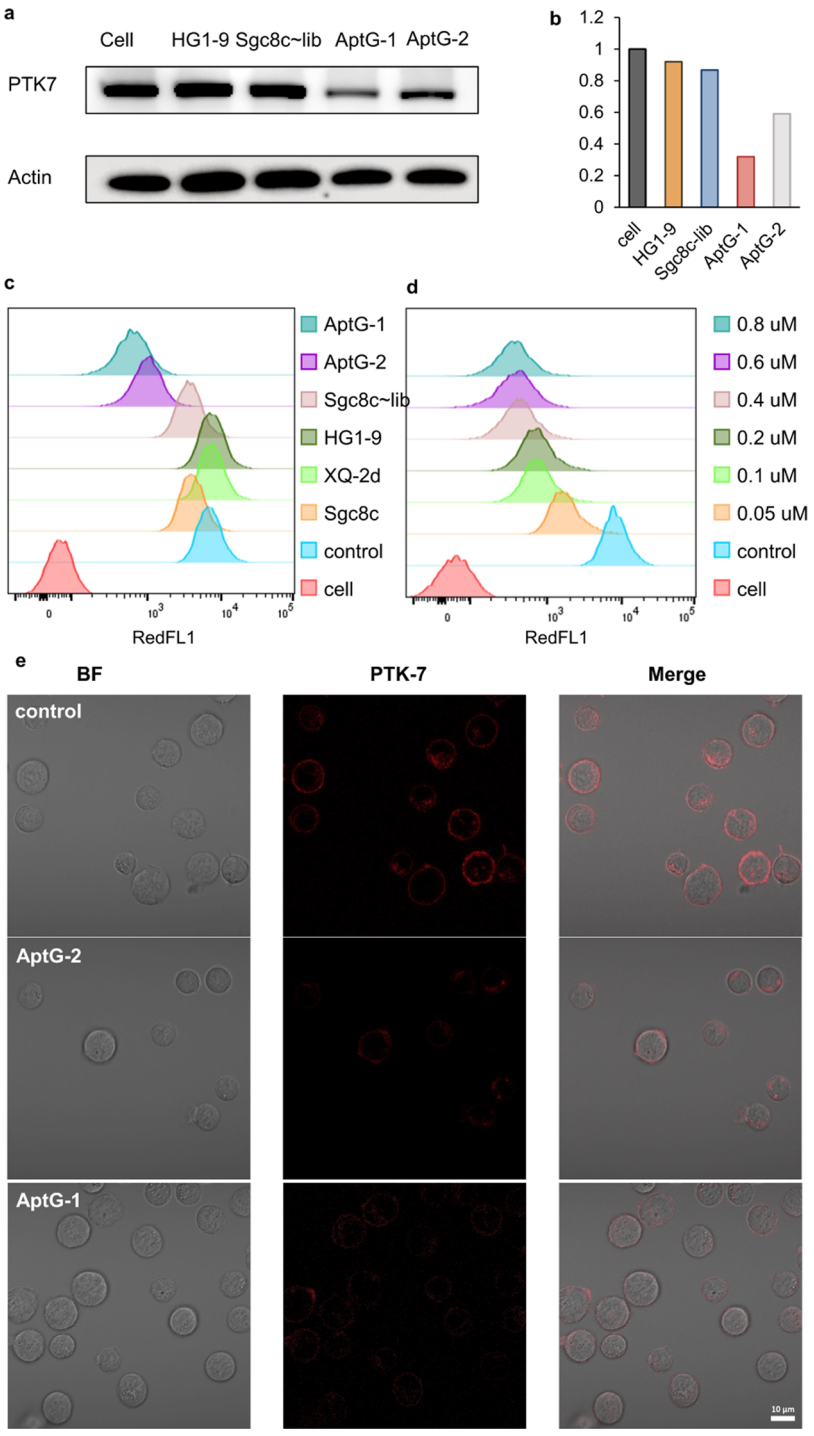

Figure 4. AptG-1 degrades PTK7 protein. (a) Determination of the PTK7 protein by western blot after treatment with 500 nM AptG-1, AptG-2, Sgc8c ~ lib, and HG1−9 aptamer for 1 h in CCRF-CEM cells. (b) Quantification of PTK7 proteins in (a). (c) Determination of PTK7 levels on CCRF-CEM cell membranes post-incubation with AptGs and aptamers by flow cytometry. Cells were incubated with 500 nM AptG-1, AptG-2, Sgc8c ~ lib, HG1−9, XQ-2d, and Sgc8c for 1 h at 37 °C, followed by adding Cy5-Sgc8c aptamer at 4 °C for 30 min. (d) Determination of PTK7 levels on membrane post-incubation with varying concentrations of AptG-1 for 1 h. (e) Determination of PTK7 levels on membrane post-incubation with control sample, and 500 nM AptG-1 and AptG-2 for 1 h at 37 °C, confocal imaging.

AptG-1 exhibited binding to and entering CCRF-CEM cells as early as 3 min, with significantly increased intracellular fluorescence intensity at 5 min, indicating a notable endocytosis tendency within such a short time frame. By the 10 min mark, a substantial amount of AptG-1 was observed to be internalized into the lysosomes (Figure 2d). In contrast, AptG-2 and Sgc8c ~ lib displayed no internalization events when incubated with CCRF-CEM cells for the same duration (Figure 2e,f).

To gain insights into why the TMPDS composed of AptG-1 and TfR1 possesses a much greater endocytosis rate, we next turned our attention to carry out mechanistic studies, including the comparison of the binding ability of AptG-1, AptG-2, HG1−9, and XQ-2d with Sgc8c, as well as identifying the endocytosis

https://doi.org/10.1021/jacsau.4c00260
JACS Au 2024, 4, 2907−2914

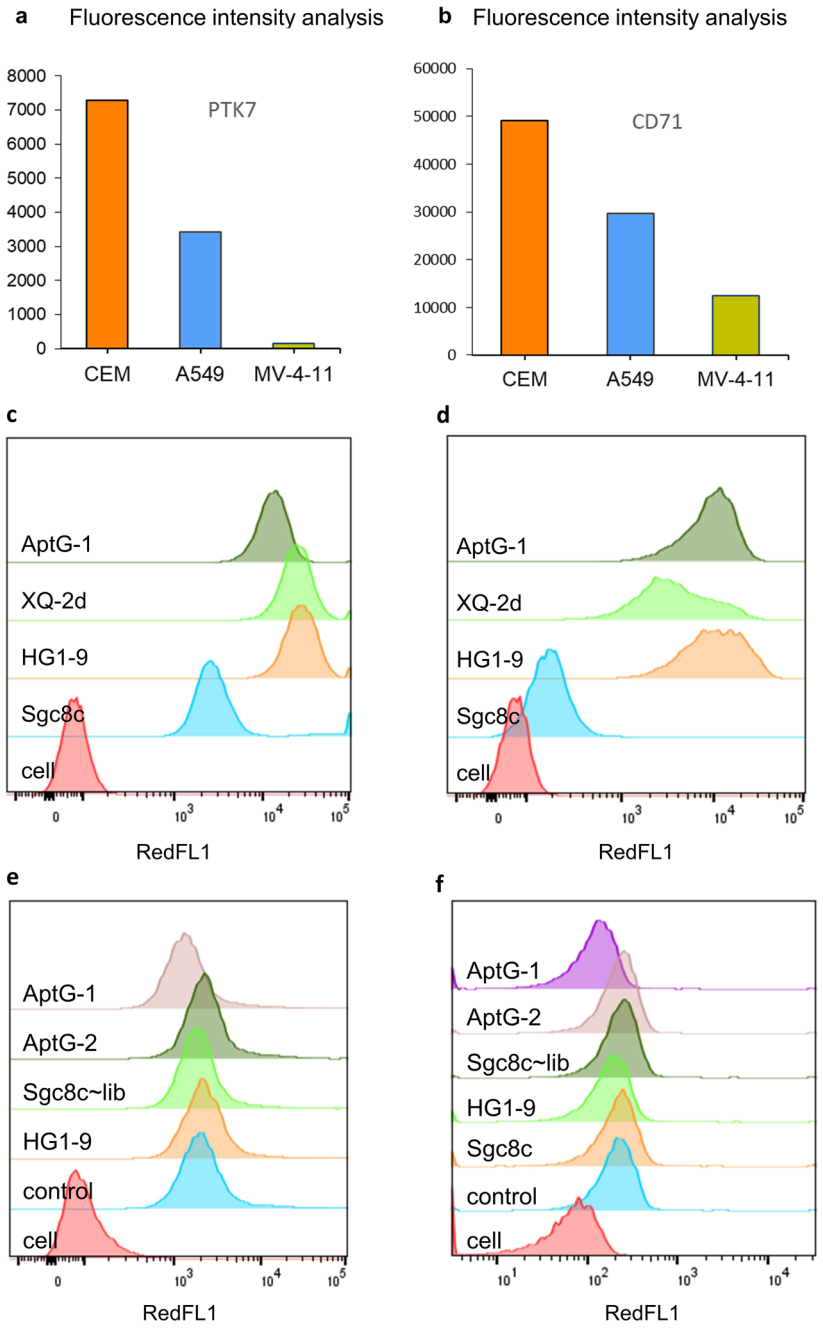

Figure 5. (a) Comparison of PTK7 protein expressions on membranes of CCRF-CEM, A549, and MV-4−11 cells. 200 nM Cy5-Sgc8c was incubated with CEM, MV-4−11, and A549 for 30 min at 4 °C. (b) Comparison of CD71 protein expressions on membranes of CCRF-CEM, A549, and MV-4−11 cells. 200 nM Cy5-HG1−9 was incubated with CEM, MV-4−11, and A549 for 30 min at 4 °C. (c) Comparison of the binding ability of aptamers against that of A549 cells. A549 cells were incubated with 200 nM AptG-1, XQ-2d, HG1−9, and Sgc8c for 30 min in binding buffer at 4 °C. (d) Comparison of the binding ability of aptamers against MV-4−11 cells. MV-4−11 cells were incubated with 200 nM AptG-1, XQ-2d, HG1−9, and Sgc8c for 30 min in binding buffer at 4 °C. (e) Determination of the superior PTK7 degradation ability of AptG-1 over other aptamers against A549 cells by flow cytometry. A549 cells were incubated with 500 nM concentrations of AptG-1, AptG-2, Sgc8c~lib, and HG1−9 in cell culture medium for 6 h at 37 °C. Subsequently, PTK7 was labeled with Cy5-Sgc8c for 30 min at 4 °C. (f) Determination of the superior PTK7 degradation ability of AptG-1 over other aptamers against MV-4−11 cells by flow cytometry. A549 cells were incubated with 500 nM concentrations of AptG-1, AptG-2, Sgc8c~lib, HG1−9, and Sgc8c for 6 h at 37 °C, followed by labeling the PTK7 receptor with Cy5-Sgc8c aptamer at 4 °C for 30 min.

pathways of AptG-1, AptG-2, and Sgc8c ~ lib. As indicated in Figure 3a,b, by co-incubating AptGs with Cy5-Sgc8c or FAM-HG1−9, AptG-1 could still efficiently bind to CCRF-CEM, forming a stable TMPDS. By contrast, a certain amount of AptG-2 fell off from the cells, revealing that the AptG-2 was not able to form a stable TMPDS as AptG-1, thus indicating that AptG-1 possesses a superior binding ability over AptG-2. Moreover, we compared the fluorescence intensity of three probes, AptG-1, AptG-2, and Sgc8c ~ lib, after incubating with CCRF-CEM cells at 4 °C for 30 min at different concentrations ranging from 0.1 to 50 nM (Figures 3c and S1). We found that the fluorescence intensity of AptG-1 was 6 times that of AptG-2 at an extremely low concentration (0.1 nM), and at a high concentration (50 nM), it was still twice that of AptG-2. In the

https://doi.org/10.1021/jacsau.4c00260
JACS Au 2024, 4, 2907−2914

replacement experiments, it was found that AptG-1 could replace the Cy5-labeled Sgc8c aptamer that binds to CCRF-CEM cells to form a TMPDS as indicated by the significantly lowered fluorescence intensity (Figure 3d). These results collectively indicate that AptG-1 can efficiently recognize and bind to target proteins.

Given the rapid internalization rate of AptG-1, we developed a keen interest in the pathways through which the TMPDS enters the cells. Reports suggest that the transport of iron ions is initiated by the endocytosis of the TfR1-transferrin complex, entering the endosome through receptor-mediated internalization pathways, then fusing with lysosomes to release iron ions in acidic conditions.[13] To demonstrate whether our TMPDS enters cells through different pathways,[14] we conducted transport inhibition experiments by adding various inhibitors, including phagocytosis, macrophagy, clathrin-mediated, and vesicle-dependent pathways (Figures 3e and S3).[15−19] We found that when chlorpromazine was used to inhibit clathrin-mediated endocytosis, the fluorescence intensity of AptG-1, AptG-2, and Sgc8c ∼ lib for CCRF-CEM cells slightly decreased (Figure 3e), suggesting that our probes may also undergo internalization via clathrin-mediated pathways. Therefore, the synergistic internalization of TfR1 and clathrin enhances the rapid endocytic action of AptG-1. These findings highlight the crucial role of the selected TfR1 ligand, conferring not only better stability and recognition capability to AptGs but also accelerating the endocytic rate of the entire TMPDS.

Having verified the recognition capability, binding affinity, and faster endocytic rate of AptG-1 in comparison to AptG-2, we conducted an in-depth investigation into the potential of our AptG-1-TfR1 TMPDS to efficiently degrade the lysosomal target protein PTK7.[1−5] To commence this exploration, we probed the endocytosis kinetics of AptG-1 using the confocal microscopy technique, revealing its rapid internalization ability (Figure S3). Subsequently, western blot analysis was employed to scrutinize alterations in the target protein on the cell membrane, with AptG-1, AptG-2, Sgc8c ∼ lib, and HG1−9 individually co-incubated with CCRF-CEM cells at 37 °C for 1 h. As illustrated in Figure 4a,b, the cells treated with AptG-1 displayed a notable reduction in PTK7 levels on the cell membrane compared to those treated with AptG-2 and Sgc8c ∼ lib. This underscores the pronounced efficacy of AptG-1 in degrading the target protein. To further substantiate the superior protein degradation efficiency of the newly developed AptG-1-TfR1 TMPDS, flow cytometry was utilized to analyze the binding kinetics of Cy5-Sgc8c on CCRF-CEM cells. Cells were pretreated with 0.5 μM AptG-1, AptG-2, Sgc8c ∼ lib, HG1−9, XQ-2d, Sgc8c, and control samples for 1 h, followed by co-incubation with 200 nM Cy5-Sgc8c at 4 °C for 30 min, as shown in Figure 4c. Remarkably, cells treated with AptG-1 exhibited the lowest fluorescence intensity in flow cytometry, indicative of the effective degradation of the PTK7 protein. Furthermore, when CCRF-CEM cells were incubated with different concentrations of AptG-1 (ranging from 50 to 800 nM) for 1 h, the binding kinetics of Cy5-Sgc8c with cells significantly decreased (Figures 4d and S4).

To provide further empirical support for the superior target protein degradation capability of the AptG-1-TfR1 TMPDS, preincubation with AptG-1, AptG-2, and Sgc8c∼lib was followed by evaluating the membrane-associated PTK7 protein content through the fluorescence signal of Cy5-Sgc8c. As depicted in Figure 4e, the fluorescence signal was weakest in the AptG-1 group, indicating efficient protein degradation. In contrast, the AptG-2 group exhibited a relatively stronger signal, while the Sgc8c ∼ lib group showed the strongest signal. These findings robustly align with the observations in Figure 2a and underscore the AptG-1-TfR1 TMPDS efficient degradation of the target protein.

To further validate the unique multifunctionality of the AptG-1-TfR1 TMPDS, we expanded our study to A549 cells (lung cancer cell line, moderate expression levels of PTK7 and CD71, as shown in Figure 5a,b),[20] MDA-MB-231 (triple-negative breast cancer cell line, moderate expression levels of PTK7 and CD71, as shown in Figure S5a),[21] and MV-4−11 (acute myeloid leukemia cell line, lowest expression levels of PTK7 and CD71, Figure 5a,b).[22] Considering the discernible impact of AptG-1 ∼ TfR1 TMPDS on the degradation of PTK7 within the CCRF-CEM cell membrane, we hypothesized its efficacy in selectively targeting and degrading PTK7 across diverse cellular contexts, including A549, MDA-MB-231, and MV-4−11, irrespective of variations in PTK7 expression levels. In the initial phase of our investigation, we systematically assessed the binding interactions of Sgc8c, HG1−9, XQ-2d, and AptG-1 with A549, MV-4−11, and MDA-MB-231 cellular entities using flow cytometry analysis (Figures 5c,d and S5a). The results revealed a pronounced binding affinity of Sgc8c for A549, surpassing that observed for MV-4−11, aligning consistently with the outcomes depicted in Figure 5a. Concurrently, AptG-1 exhibited a robust binding propensity with the A549 and MV-4−11 cell lines. This empirical insight establishes a solid foundation for our subsequent utilization of AptG-1 ∼ TfR1 TMPDS to facilitate the targeted degradation of specific proteins. To rigorously validate the system's proficiency in selectively degrading PTK7, we employed flow cytometry analysis. As delineated in Figures 5e,f, and S5b,c, the noticeable reduction in the binding trend of Cy5-Sgc8c in the AptG-1-treated group, subsequent to preincubation with cells, unequivocally affirms the system's adeptness in efficiently degrading PTK7 within the cellular membranes of A549 and MV-4−11 cell lines. However, we also observed that our TMPDS does not work well for the MDA-MB-231 cell line, and we currently do not have an explanation for this result.

In conclusion, our study presents a highly efficient TMPDS that significantly advances the field of molecular medicine. By leveraging a novel combination of a bivalent aptamer glue and a protein transport shuttle, we demonstrated the system's ability to effectively degrade the protein tyrosine kinase 7 (PTK7) in CCRF-CEM cells and target lowly expressed PTK7 in MV-4−11 cells. These results not only underscore the TMPDS' broad applicability and multifunctionality but also establish a strong foundation for its potential in diverse therapeutic interventions and the exploration of cellular mechanisms.

■ ASSOCIATED CONTENT

Supporting Information

The Supporting Information is available free of charge at https://pubs.acs.org/doi/10.1021/jacsau.4c00260.

Construction of AptGs; stability determination; procedures for cell-associated experiments, including flow cytometry, etc.; and westen blot (PDF)

■ AUTHOR INFORMATION

Corresponding Author

Xue-Qiang Wang − *Molecular Science and Biomedicine Laboratory (MBL), State Key Laboratory of Chemo/*

https://doi.org/10.1021/jacsau.4c00260
JACS Au 2024, 4, 2907−2914

Biosensing and Chemometrics, College of Chemistry and Chemical Engineering, Aptamer Engineering Center of Hunan Province, Hunan University, Changsha, Hunan 410082, China; The Key Laboratory of Zhejiang Province for Aptamers and Theranostics, Zhejiang Cancer Hospital, Hangzhou Institute of Medicine (HIM), Chinese Academy of Sciences, Hangzhou, Zhejiang 310022, China; orcid.org/0000-0003-1631-9158; Email: wangxq@hnu.edu.cn

Authors

Guo-Rong Zhang − *Molecular Science and Biomedicine Laboratory (MBL), State Key Laboratory of Chemo/Biosensing and Chemometrics, College of Chemistry and Chemical Engineering, Aptamer Engineering Center of Hunan Province, Hunan University, Changsha, Hunan 410082, China*

Chi Zhang − *Molecular Science and Biomedicine Laboratory (MBL), State Key Laboratory of Chemo/Biosensing and Chemometrics, College of Chemistry and Chemical Engineering, Aptamer Engineering Center of Hunan Province, Hunan University, Changsha, Hunan 410082, China*

Ting Fu − *The Key Laboratory of Zhejiang Province for Aptamers and Theranostics, Zhejiang Cancer Hospital, Hangzhou Institute of Medicine (HIM), Chinese Academy of Sciences, Hangzhou, Zhejiang 310022, China*

Weihong Tan − *Molecular Science and Biomedicine Laboratory (MBL), State Key Laboratory of Chemo/Biosensing and Chemometrics, College of Chemistry and Chemical Engineering, Aptamer Engineering Center of Hunan Province, Hunan University, Changsha, Hunan 410082, China; The Key Laboratory of Zhejiang Province for Aptamers and Theranostics, Zhejiang Cancer Hospital, Hangzhou Institute of Medicine (HIM), Chinese Academy of Sciences, Hangzhou, Zhejiang 310022, China; Institute of Molecular Medicine (IMM), Renji Hospital, School of Medicine, College of Chemistry and Chemical Engineering, Shanghai Jiao Tong University, Shanghai 200127, China;* orcid.org/0000-0002-8066-1524

Complete contact information is available at: https://pubs.acs.org/10.1021/jacsau.4c00260

Notes

The authors declare no competing financial interest.

■ ACKNOWLEDGMENTS

This work was supported by the National Key Research and Development Program of China (no. 2023YFC3402900); the National Natural Science Foundation of China (21991080); Hunan Provincial Science Foundation for Distinguished Young Scholars (2022JJ10005); and Key Science and Technology project of Hunan Province (2021SK1020).

■ REFERENCES

(1) Banik, S. M.; Pedram, K.; Wisnovsky, S.; Ahn, G.; Riley, N. M.; Bertozzi, C. R. Lysosome-targeting chimaeras for degradation of extracellular proteins. *Nature* **2020**, *584*, 291−297.

(2) Zhang, H.; Han, Y.; Yang, Y.; Lin, F.; Li, K.; Kong, L.; Liu, H.; Dang, Y.; Lin, J.; Chen, P. R. Covalently Engineered Nanobody Chimeras for Targeted Membrane Protein Degradation. *J. Am. Chem. Soc.* **2021**, *143*, 16377−16382.

(3) Cotton, A. D.; Nguyen, D. P.; Gramespacher, J. A.; Seiple, I. B.; Wells, J. A. Development of Antibody-Based PROTACs for the Degradation of the Cell-Surface Immune Checkpoint Protein PD-L1. *J. Am. Chem. Soc.* **2021**, *143*, 593−598.

(4) Miao, Y.; Gao, Q.; Mao, M.; Zhang, C.; Yang, L.; Yang, Y.; Han, D. Bispecific Aptamer Chimeras Enable Targeted Protein Degradation on Cell Membranes. *Angew. Chem., Int. Ed.* **2021**, *60*, 11267−11271.

(5) Liu, Y.; Qian, X.; Ran, C.; Li, L.; Fu, T.; Su, D.; Xie, S.; Tan, W. Aptamer-Based Targeted Protein Degradation. *ACS Nano* **2023**, *17*, 6150−6164.

(6) Daniels, T. R.; Delgado, T.; Rodriguez, J. A.; Helguera, G.; Penichet, M. L. The transferrin receptor part I: Biology and targeting with cytotoxic antibodies for the treatment of cancer. *Clin. Immunol.* **2006**, *121*, 144−158.

(7) Uhlén, M.; Fagerberg, L.; Hallström, B. M.; Lindskog, C.; Oksvold, P.; Mardinoglu, A.; Sivertsson, Å.; Kampf, C.; Sjöstedt, E.; Asplund, A.; Olsson, I.; Edlund, K.; Lundberg, E.; Navani, S.; Szigyarto, C. A.; Odeberg, J.; Djureinovic, D.; Takanen, J. O.; Hober, S.; Alm, T.; Edqvist, P. H.; Berling, H.; Tegel, H.; Mulder, J.; Rockberg, J.; Nilsson, P.; Schwenk, J. M.; Hamsten, M.; von Feilitzen, K.; Forsberg, M.; Persson, L.; Johansson, F.; Zwahlen, M.; von Heijne, G.; Nielsen, J.; Pontén, F. Proteomics. Tissue-based map of the human proteome. *Science* **2015**, *347*, No. 1260419, DOI: 10.1126/science.1260419.

(8) Wu, X.; Liu, H.; Han, D.; Peng, B.; Zhang, H.; Zhang, L.; Li, J.; Liu, J.; Cui, C.; Fang, S.; Li, M.; Ye, M.; Tan, W. Elucidation and Structural Modeling of CD71 as a Molecular Target for Cell-Specific Aptamer Binding. *J. Am. Chem. Soc.* **2019**, *141*, 10760−10769.

(9) Zhang, N.; Bing, T.; Shen, L.; Feng, L.; Liu, X.; Shangguan, D. A DNA Aptameric Ligand of Human Transferrin Receptor Generated by Cell-SELEX. *Int. J. Mol. Sci.* **2021**, *22*, No. 8923, DOI: 10.3390/ijms22168923.

(10) Lu, X.; Borchers, A. G.; Jolicoeur, C.; Rayburn, H.; Baker, J. C.; Tessier-Lavigne, M. PTK7/CCK-4 is a novel regulator of planar cell polarity in vertebrates. *Nature* **2004**, *430*, 93−98.

(11) Shangguan, D.; Tang, Z.; Mallikaratchy, P.; Xiao, Z.; Tan, W. Optimization and modifications of aptamers selected from live cancer cell lines. *Chembiochem* **2007**, *8*, 603−606.

(12) Zhang, G.-R.; Tan, W.; Wang, X.-Q. Chemical Tailoring of Aptamer Glues with Significantly Enhanced Recognition Ability for Targeted Membrane Protein Degradation. *ACS Nano* **2023**, *17*, 15146−15154.

(13) Drakesmith, H.; Nemeth, E.; Ganz, T. Ironing out Ferroportin. *Cell Metab.* **2015**, *22*, 777−787.

(14) Doherty, G. J.; McMahon, H. T. Mechanisms of endocytosis. *Annu. Rev. Biochem.* **2009**, *78*, 857−902.

(15) Kaksonen, M.; Roux, A. Mechanisms of clathrin-mediated endocytosis. *Nat. Rev. Mol. Cell Biol.* **2018**, *19*, 313−326.

(16) Sinha, B.; Köster, D.; Ruez, R.; Gonnord, P.; Bastiani, M.; Abankwa, D.; Stan, R. V.; Butler-Browne, G.; Vedie, B.; Johannes, L.; Morone, N.; Parton, R. G.; Raposo, G.; Sens, P.; Lamaze, C.; Nassoy, P. Cells respond to mechanical stress by rapid disassembly of caveolae. *Cell* **2011**, *144*, 402−413.

(17) Gordon, S. Phagocytosis: An Immunobiologic Process. *Immunity* **2016**, *44*, 463−475.

(18) Koivusalo, M.; Welch, C.; Hayashi, H.; Scott, C. C.; Kim, M.; Alexander, T.; Touret, N.; Hahn, K. M.; Grinstein, S. Amiloride inhibits macropinocytosis by lowering submembranous pH and preventing Rac1 and Cdc42 signaling. *J. Cell Biol.* **2010**, *188*, 547−563.

(19) Shen, W. J.; Azhar, S.; Kraemer, F. B. SR-B1: A Unique Multifunctional Receptor for Cholesterol Influx and Efflux. *Annu. Rev. Physiol.* **2018**, *80*, 95−116.

(20) Raivola, J.; Dini, A.; Karvonen, H.; Piki, E.; Salokas, K.; Niininen, W.; Kaleva, L.; Zhang, K.; Arjama, M.; Gudoityte, G.; Seashore-Ludlow, B.; Varjosalo, M.; Kallioniemi, O.; Hautaniemi, S.; Murumägi, A.; Ungureanu, D. Multiomics characterization implicates PTK7 in ovarian cancer EMT and cell plasticity and offers strategies for therapeutic intervention. *Cell Death Dis.* **2022**, *13*, No. 714, DOI: 10.1038/s41419-022-05161-5.

(21) Damelin, M.; Bankovich, A.; Bernstein, J.; Lucas, J.; Chen, L.; Williams, S.; Park, A.; Aguilar, J.; Ernstoff, E.; Charati, M.; Dushin, R.; Aujay, M.; Lee, C.; Ramoth, H.; Milton, M.; Hampl, J.; Lazetic, S.;

Pulito, V.; Rosfjord, E.; Sun, Y.; King, L.; Barletta, F.; Betts, A.; Guffroy, M.; Falahatpisheh, H.; O'Donnell, C. J.; Stull, R.; Pysz, M.; Escarpe, P.; Liu, D.; Foord, O.; Gerber, H. P.; Sapra, P.; Dylla, S. J. A PTK7-targeted antibody-drug conjugate reduces tumor-initiating cells and induces sustained tumor regressions. *Sci. Transl. Med.* **2017**, *9*, No. eaag26119.

(22) Li, K.; Chen, C.; Gao, R.; Yu, X.; Huang, Y.; Chen, Z.; Liu, Z.; Chen, S.; Luo, G.; Huang, X.; Przybylski, G. K.; Li, Y.; Zeng, C. Inhibition of BCL11B induces downregulation of PTK7 and results in growth retardation and apoptosis in T-cell acute lymphoblastic leukemia. *Biomarker Res.* **2021**, *9*, No. 17, DOI: 10.1186/s40364-021-00270-3.

https://doi.org/10.1021/jacsau.4c00260
JACS Au 2024, 4, 2907−2914